Amorphous $CoMoO_4$ with Nanoporous Structure for Electrochemical Ammonia Synthesis under Ambient Conditions

*Lin Xiao[a], Yanqin Liang[a, b], Zhaoyang Li[a, b],Shuilin Wu[a, b], Shengli Zhu[a,b ,d, *],*

*Shuiyuan Luo[d], Chuntao Chang[e, *], Zhenduo Cui[a, b, *]*

a School of Materials Science and Engineering, Tianjin University, Tianjin, 300350, China

b Key Laboratory of Advanced Ceramics and Machining Technology, Ministry of Education, Tianjin, 300350, China

c School of Materials Science and Engineering, Lanzhou Jiaotong University, Lanzhou, 730070, China

d College of Chemistry Engineering and Materials Science, Quanzhou Normal University, Quanzhou, 362000, Fujian, China

e School of Mechanical Engineering, Dongguan University of Technology, Dongguan, 523808, China

*Corresponding Authors.

E-mail address: slzhu@tju.edu.cn. changct@dgut.edu.cn. zdcui@tju.edu.cn

Number of pages: 9

Number of figures: 14

Number of tables: 1

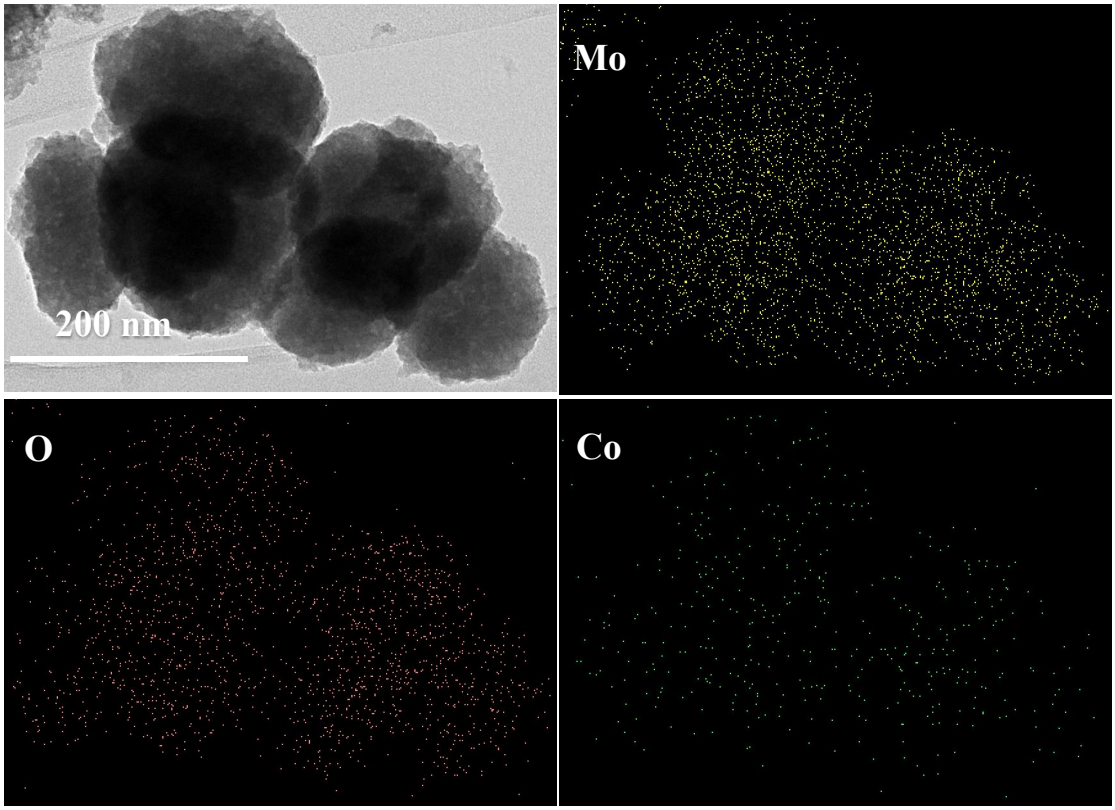

Figure S1. EDX element mapping images of $CoMoO_4$.

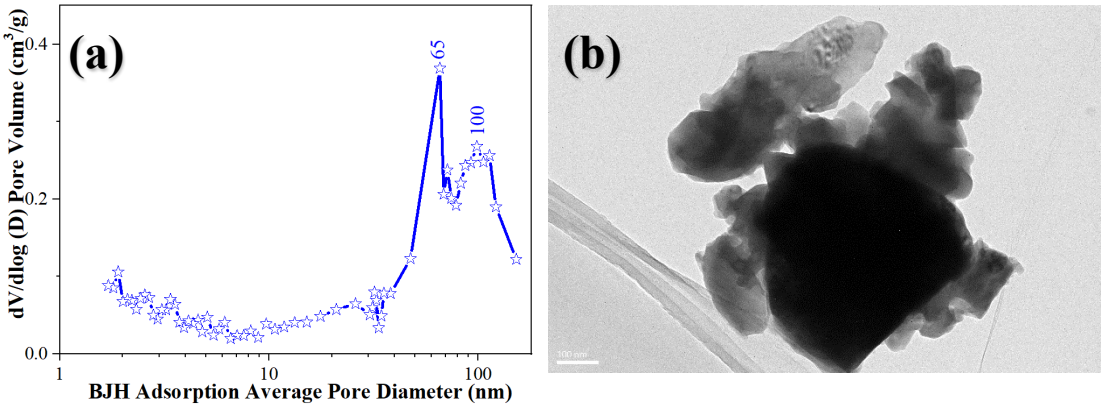

Figure S2. (a) BJH adsorption average pore diameter of amorphous $CoMoO_4$ catalyst.

(b)TEM image of crystal $CoMoO_4$ catalyst.

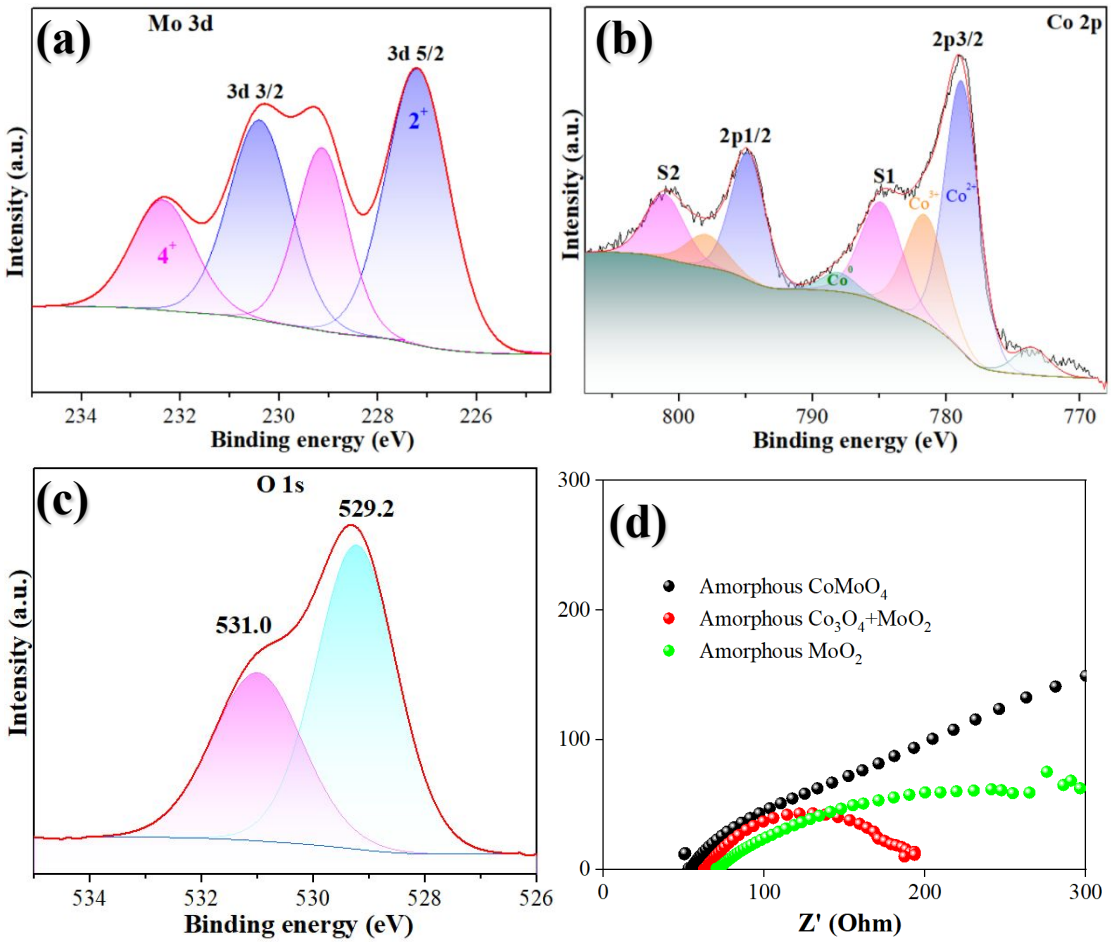

Figure S3. XPS spectra of mixture (MoO_2 + Co_3O_4) for (a) Mo 3d and (b) Co 2p (c) O 1s, (d) Nyquist plots of amorphous $CoMoO_4$, amorphous Co_3O_4+MoO_2 and amorphous MoO_2.

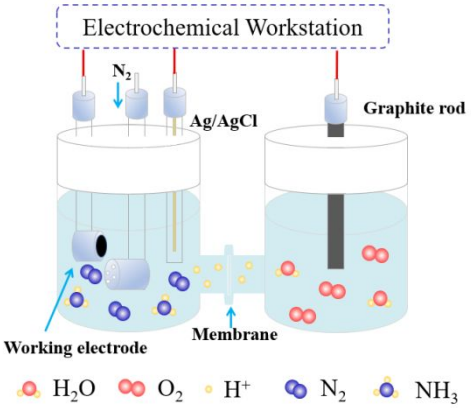

Figure S4. The schematic of electrolytic cell.

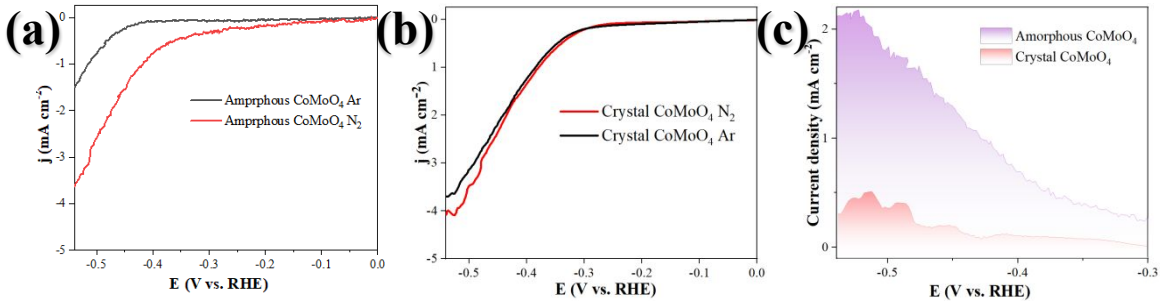

Figure S5. LSV curves of (a) amorphous $CoMoO_4$ and (b) crystal $CoMoO_4$ under N_2 and Ar, (c) Net current density.

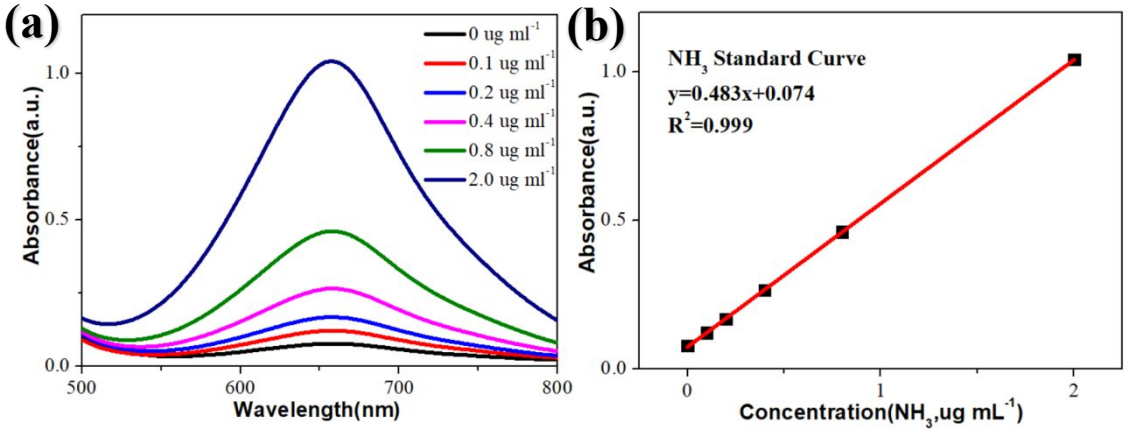

Figure S6. (a) UV-Vis spectrum of different NH_4^+ content by indophenol assays after incubated for 2 h at room temperature. (b) Calibration curve used for the estimation of NH_4^+ concentration.

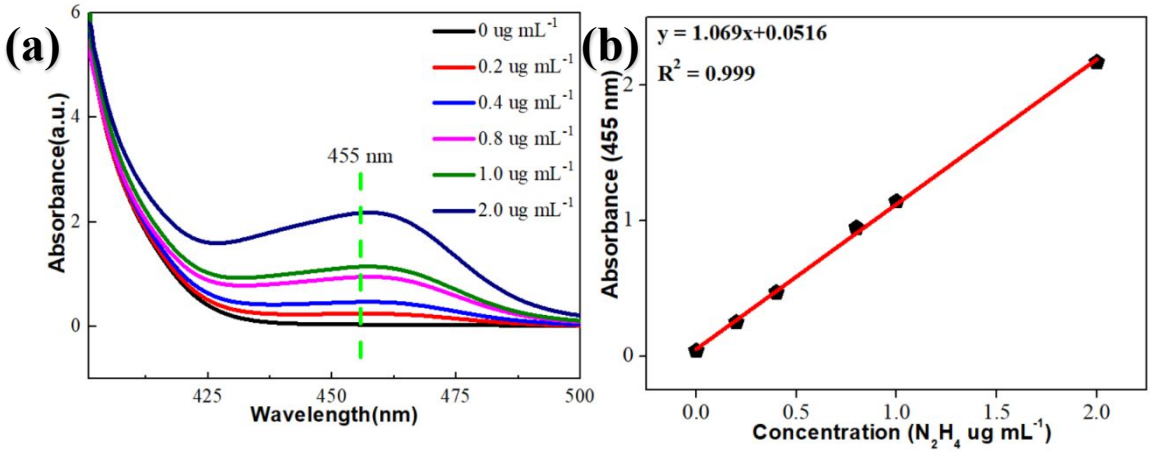

Figure S7. (a) UV-Vis spectra of different N_2H_4 content after incubated for 15 min at room temperature. (b) Calibration curve used for calculation of N_2H_4 concentration.

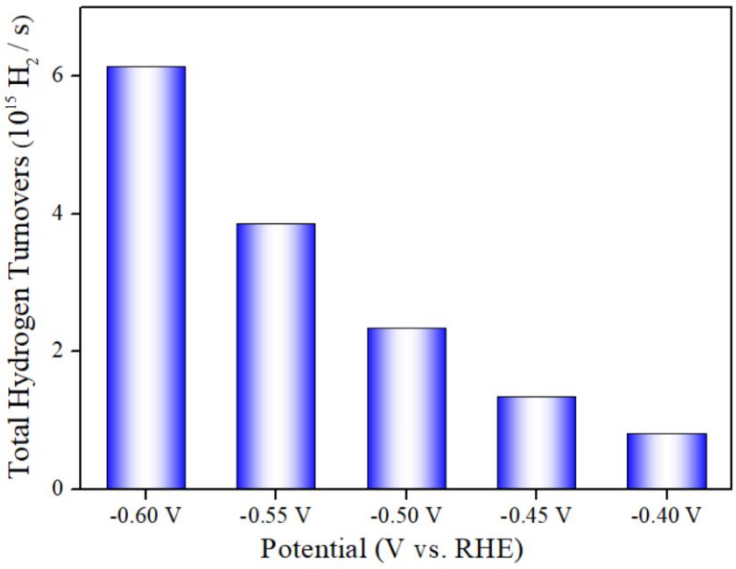

Figure S8. The total hydrogen turnovers at each given potential.

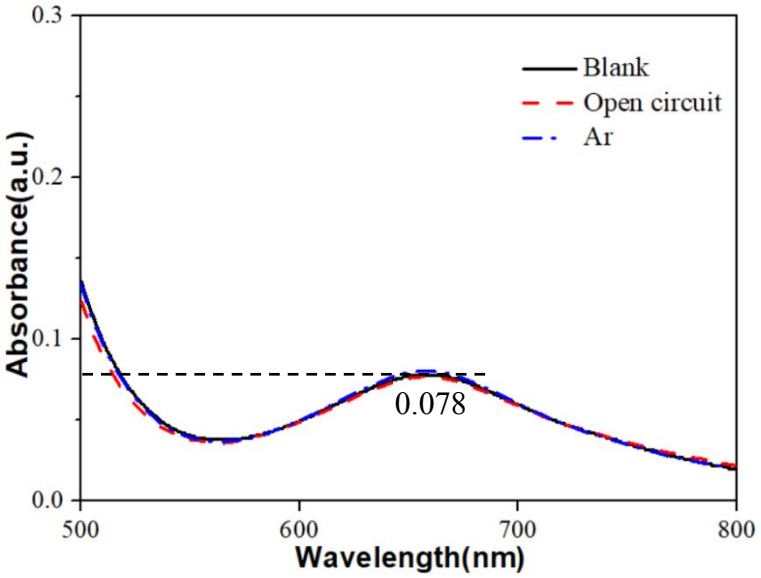

Figure S9. UV-Vis spectra of the electrolytes for blank ground, supplying N_2 for 2 h with no applied voltage and supplying Ar for 2 h electrolysis at -0.50 V.

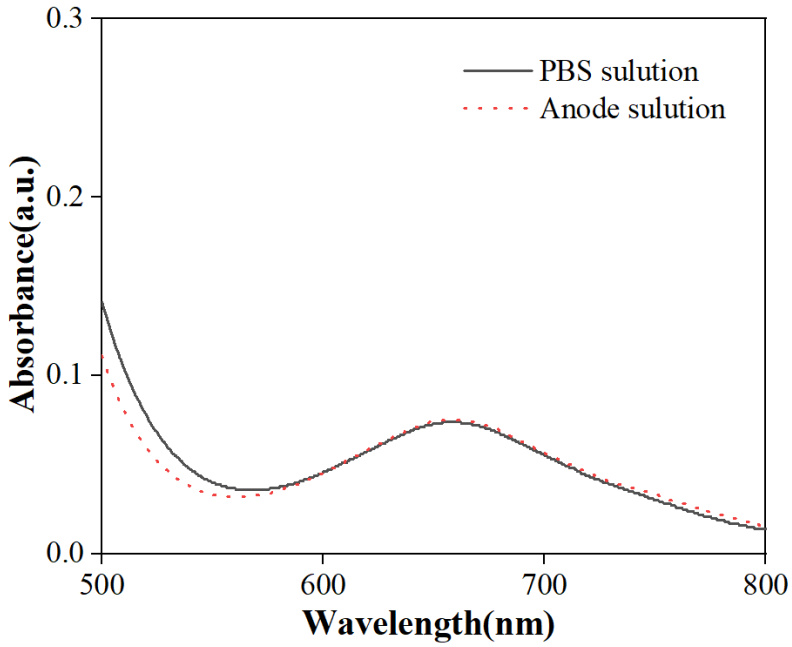

Figure S10. UV-Vis spectra of the PBS solution and anode electrolyte after NRR.

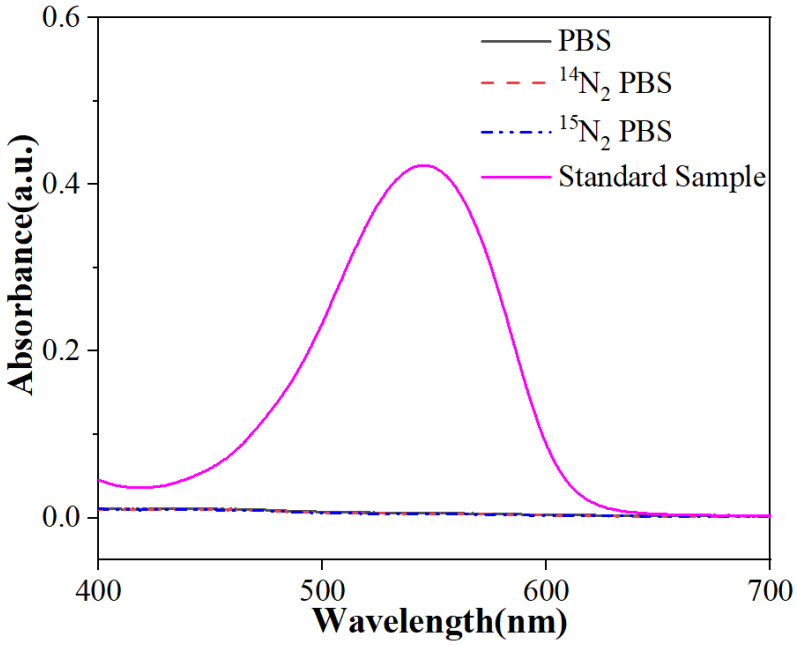

Figure S11. UV-vis adsorption spectra of nitrite detection

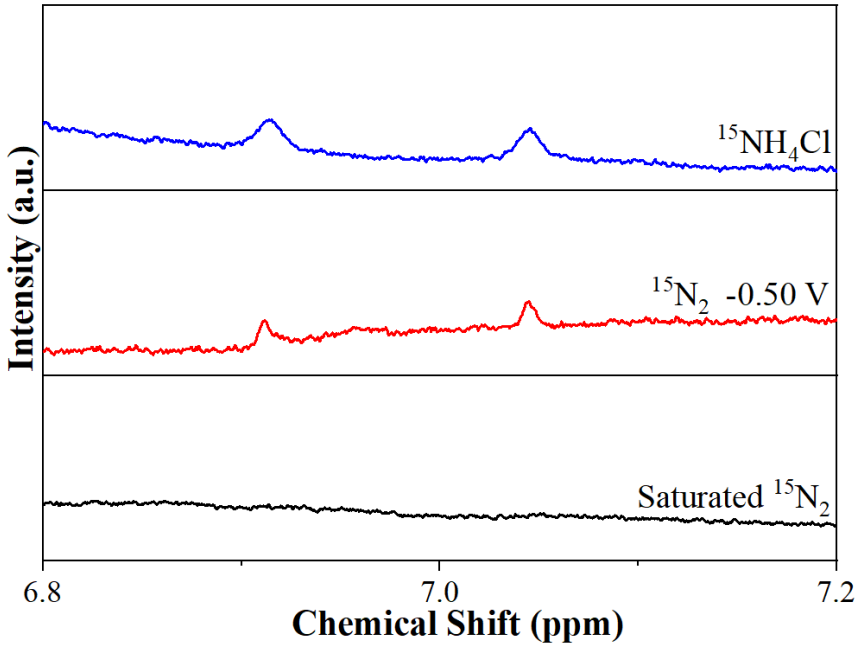

Figure S12. The ^{1}H NMR spectra of $^{15}NH_4Cl$, NRR test under $^{15}N_2$ at -0.50 V and saturated $^{15}N_2$ solution.

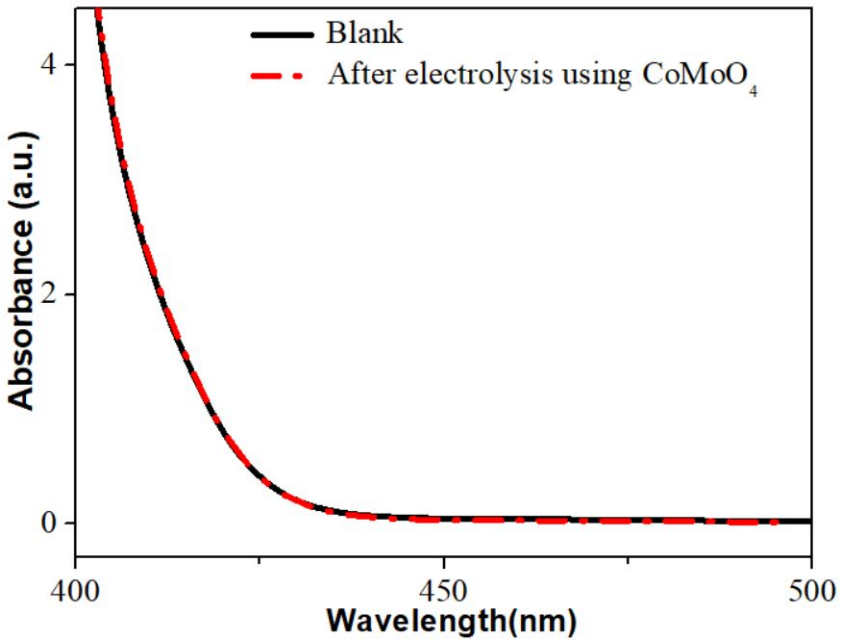

Figure S13. UV-Vis spectrum of N_2H_4 detection before and after 2 h electrolysis using amorphous $CoMoO_4$ sphere at -0.50 V.

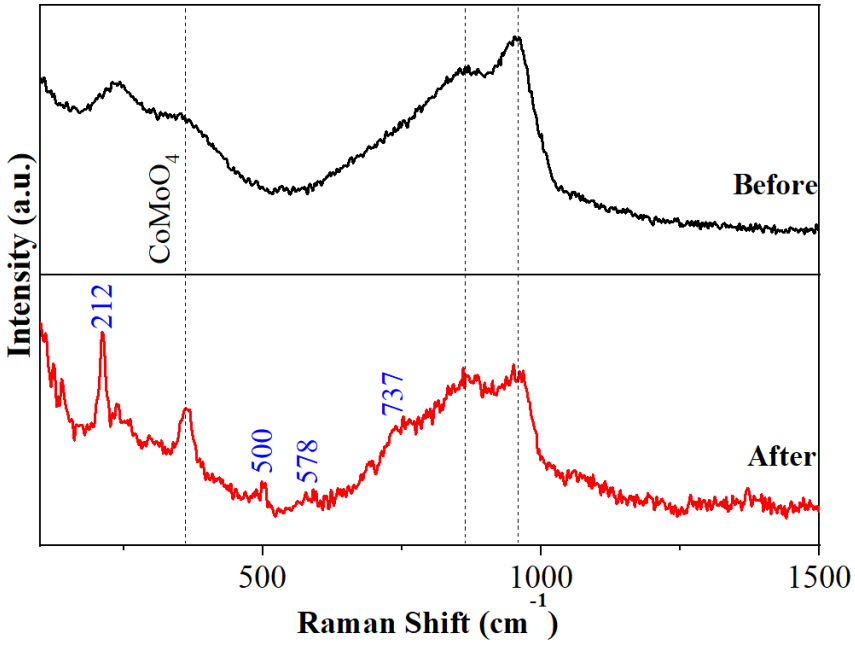

Figure S14. The Raman spectra of samples before and after stability test.

Table S1. Comparison of the electrocatalytic NRR performance of amorphous $CoMoO_4$ with other Mo-based and oxides electrocatalysts.

Catalyst	Electrolyte	V_{NH3} (ug h^{-1} mg_{cat}^{-1})	FE(%)	Ref.
$CoMoO_4$	0.1 M PBS	30.2	3.8	This work
O-MoC	0.1 mM HCl + 0.5 M Li_2SO_4	22.5	25.1	ACS Appl. Mater. Interfaces 2019, 11, 31869−31877
PdCu/rGO	0.1 m KOH	2.8	3	Adv. Energy Mater. 2018, 8, 1800124
NbO_2	0.05 m H_2SO_4	11.6	32	Small Methods 2018, 1800386
$LaCrO_3$	0.1 M Na_2SO_4	24.8	15	ChemCatChem 2019, 11, 1–6
$LaFeO_3$	2 M KOH 80 ℃	13.46	1.99	Ind. Eng. Chem. Res. 2019, 58, 8935−8939
$LiMn_2O_4$	0.1 M HCl	15.83	0.72	Inorg. Chem. 2019, 58, 9597−9601
Bi_2MoO_6	0.1 M HCl	20.46	8.17	ACS Sustainable Chem. Eng. 2019, 7, 12692−12696
$Fe_2(MoO_4)_3$	0.1 M Na_2SO_4	18.16	9.1	ASC Sunstainable Chem. Eng. 7 (2019) 12692-12696.
MoS_2	0.1 M Na_2SO_4	29.28	8.34	Adv. Energy Mater. 2018, 1801357
Mn_3O_4	0.1 M Na_2SO_4	11.6	3	Small 2018, 1803111
CeO_2	0.1 M Na_2SO_4	16.4	3.7	ACS Sustainable Chem. Eng. 2019, 7, 2889−2893
NiO/G	0.1 M Na_2SO_4	18.6	7.8	ACS Appl. Energy Mater. 2019, 2, 2288−2295
Fe_2O_3	0.1 M Na_2SO_4	15.9	0.94	ChemCatChem 2018, 10, 4530–4535
V-doped TiO_2	0.5 M $LiClO_4$	17.73	15.9	Small Methods 2019, 1900356
β-Bi_2O_3	0.1 M Na_2SO_4	19.92	4.3	ChemCatChem 2019, 11, 1884–1888
Au/CoO_x	0.05 M H_2SO_4	15.1	19	Angew. Chem. Int. Ed. 2019, 58, 2–8
F-SnO_2/CC	0.1 M Na_2SO_4	19.3	8.6	Inorg. Chem. 2019, 58, 10424−10431